

Article

Surface Properties of Spray-Assisted Layer-By-Layer ElectroStatic Self-Assembly Treated Wooden Take-Off Board

Yi Wan ¹, Sijie Hou ², Mengyao Guo ³ and Yanchun Fu ^{2,4,*}¹ Department of Physical Education, Nanjing Forestry University, Nanjing 210037, China; wanyi@njfu.edu.cn² College of Furnishings and Industrial Design, Nanjing Forestry University, Nanjing 210037, China; Sijiehou@126.com³ College of Material Science and Engineering, Nanjing Forestry University, Nanjing 210037, China; gmy1336769458@163.com⁴ Co-Innovation Center of Efficient Processing and Utilization of Forest Resources, Nanjing Forestry University, Nanjing 210037, China

* Correspondence: yanchunfu@njfu.edu.cn; Tel.: +86-25-8542-7793

Abstract: Wooden take-off board is easy to crack, deform, discolor, and decay when it is used outdoors, which not only increases maintenance costs but also reduces its service life. Multifunctional coatings with UV-resistant, water-repellent, and flame-retardant properties were successfully obtained on the surface of a wooden take-off board substrate by spray-assisted layer-by-layer self-assembly. The coatings consisted of positively-charged chitosan, Al (OH)₃, and negatively-charged sodium phytate through electrostatic adsorption several times. The treated wood exhibited high UV resistance, and the color remained constant after 720 hours of ultraviolet irradiation. The wettability of the wood surface after treatment became superhydrophobic, with initial static contact angles as high as 140°. In addition, limiting oxygen index and air exposure combustion tests were used to verify that chitosan, sodium phytate, and aluminum hydroxide could synergistically confer significant fire resistance to modified wood.



Citation: Wan, Y.; Hou, S.; Guo, M.; Fu, Y. Surface Properties of Spray-Assisted Layer-By-Layer ElectroStatic Self-Assembly Treated Wooden Take-Off Board. *Appl. Sci.* **2021**, *11*, 836. <https://doi.org/10.3390/app11020836>

Received: 24 November 2020

Accepted: 15 January 2021

Published: 17 January 2021

Publisher's Note: MDPI stays neutral with regard to jurisdictional claims in published maps and institutional affiliations.



Copyright: © 2021 by the authors. Licensee MDPI, Basel, Switzerland. This article is an open access article distributed under the terms and conditions of the Creative Commons Attribution (CC BY) license (<https://creativecommons.org/licenses/by/4.0/>).

Keywords: wood surface; coating; UV-resistant; water-repellent; flame-retardant; layer-by-layer self-assembly

1. Introduction

In physical education, take-off boards are commonly used equipment, especially in the long jump and pommel horse [1]. Existing take-off boards are primarily made of pine or Chinese fir, but when used outdoors for long periods of exposure, the degradation of wood components can be accelerated by light, water, heat, microorganisms, and other natural factors. Cracking, deformation, discoloration, and decay of the wood surface not only increase the maintenance cost after use but also reduce its service life [2]. Thus, there is a need for outdoor wooden take-off boards with improved weather resistance [3–6].

Wood modification and wood finishing can be used either individually or jointly for outdoor wood protection [7,8]. The former immerses a medicament into the cellular pore structure of wood by physical filling or chemical binding to improve the properties of the wood [9–11]. However, the reagent can be easily lost, and the protective effect decreases as the exposure time of the modified wood increases. In addition to the aesthetic effect, the surface coating of wood can effectively isolate the influence of the external environment on wood [12–14]. Nevertheless, the service life of wood is short in outdoor or harsh environments as most coatings only partially improve the performance of wood.

The development of wood coatings could benefit from nanotechnological methods, such as polyelectrolyte layer-by-layer (LbL) self-assembly. Over the past few decades, electrostatic LbL assembly has been developed as a simple, practical, and versatile method [15–17]. It creates thin films with desirable layer composition (in the nanometer range) both on large

surfaces and on microfibers and cores. These LbL-assembled films on fibers result in new properties that are difficult to achieve with pulp fiber substrates [18–21]. Impregnated LbL self-assembly films have the advantage of simple equipment requirements and operational needs; however, disadvantages include the requirements of repeated impregnation, rinsing, and drying [22,23]. Moreover, the film formation is time-consuming; thus, impregnated LbL self-assembly film is a complicated procedure that has become one of the most significant bottlenecks in the development of this technology [24]. Compared with traditional impregnation methods, the spray self-assembly method can shorten the contact time between the polyelectrolyte and charged surface and does not require a drying procedure [25–27]. Polyelectrolyte sodium sulfonate (PSS) and polydimethyl dipropylene dilute ammonium chloride (PDDA) composite films were prepared for the first time by Schlenoff et al. through self-assembled spraying [28]. Therefore, the time required for film formation can be greatly shortened when making polymer films with the same number of layers.

Herein, we describe a facile spray-assisted LbL self-assembly method. Specifically, we used natural chitosan and sodium phytate as cationic and anionic electrolytes respectively to prepare multilayer composite films on the wood surface by spraying LbL electrostatic self-assembly. Compared with synthetic polyelectrolytes with high crystallinities and low melting points, which lead to narrow processing temperature ranges, low permeability, and poor interface stability, natural polyelectrolytes are highly water-soluble and have excellent adsorption abilities and interfacial stabilities [29,30]. Aluminum hydroxide ($\text{Al}(\text{OH})_3$) is known to be an excellent flame retardant and can be electrostatically adsorbed as functional groups [31,32]. However, nano aluminum hydroxide can increase the surface area of the substrate, thus increasing its hydrophobicity [33]. The photochromic resistance, wetting performance, and combustion properties of the test materials before and after treatment were analyzed by a UV-aging instrument, a contact angle tester, and a limit oxygen index instrument, respectively. The new multifunctional coatings are expected to be durable, color-preserving, ultraviolet (UV)-protected, water- and dust-repellent, non-contaminating, and easy to clean.

2. Materials and Methods

2.1. Materials

Chinese fir board formed into small blocks ($150 \times 150 \times 3$ mm) was supplied by Yihua Living Science and Technology Co., Ltd. (Shantou, China). Aluminum hydroxide (99.99% metals basis, 2–10 μm) and chitosan (high viscosity: $>400 \text{ MPa} \times \text{s}$) were purchased from Shanghai Machlin Biochemical Co., Ltd. (Shanghai, China). Sodium phytate (99.0%) was purchased from Hefei Bosf Biotechnology Co., Ltd. (Hefei, China). Hydrochloric acid (36.5–38.0%) was purchased from Nanjing Chemical Reagent Co., Ltd. (Nanjing, China). The distilled water used was obtained from a laboratory-grade ultra-purification water system (PLUS-E3-10TH, Nanjing Yipu Yida Technology Development Co., Ltd., Nanjing, China).

2.2. Fabrication of Chitosan/Sodium Phytate/ $\text{Al}(\text{OH})_3$ Coatings on the Wood Surface

Cationic chitosan solution was prepared by dissolving 1 g chitosan powder in 100 mL distilled water with a constant stirring speed until fully dissolved. The pH of the solution was adjusted to 2–3 by the dropwise addition of dilute hydrochloric acid. Anionic sodium phytate solution was obtained by dissolving 1 g phytate solution powder in 100 mL distilled water with a constant stirring speed until fully dissolved. The pH of the solution was also adjusted to 2–3 with dilute hydrochloric acid. In the same manner, a cationic aluminum hydroxide solution was prepared by dissolving 1 g aluminum hydroxide powder in 100 mL distilled water with a constant stirring speed until fully dissolved. The pH of the solution was also adjusted to 2–3 with dilute hydrochloric acid. The solutions were automatically sprayed using a self-made spraying machine onto the wood surface. The specific spraying process is shown in a schematic diagram (Figure 1). First, the configured chitosan solution

was evenly sprayed on the wood specimen surface for 60 s. Next, the specimen was transferred into the oven and dried at 80 °C for 1 h. We named the wood processed in this step as CH wood. Second, the configured sodium phytate solution was evenly sprayed on the CH wood surface for 60 s. The specimen was then transferred into the oven and dried at 80 °C for 1 h. The wood processed in this step was named CH/SP wood. Third, the configured aluminum hydroxide solution was evenly sprayed on the wood surface for 60 s. The specimen was then transferred into the oven and dried at 80 °C for 1 h. The wood processed in this step was designated as CH/SP/Al(OH)₃ wood. Next, the sodium phytate solution was sprayed and then followed by the spraying of the aluminum hydroxide solution, and this cycle was repeated alternately. To ensure complete coverage of the wood substrate, 10 deposition cycles were used for each sample. Meanwhile, untreated wood specimens were used for comparative purposes.

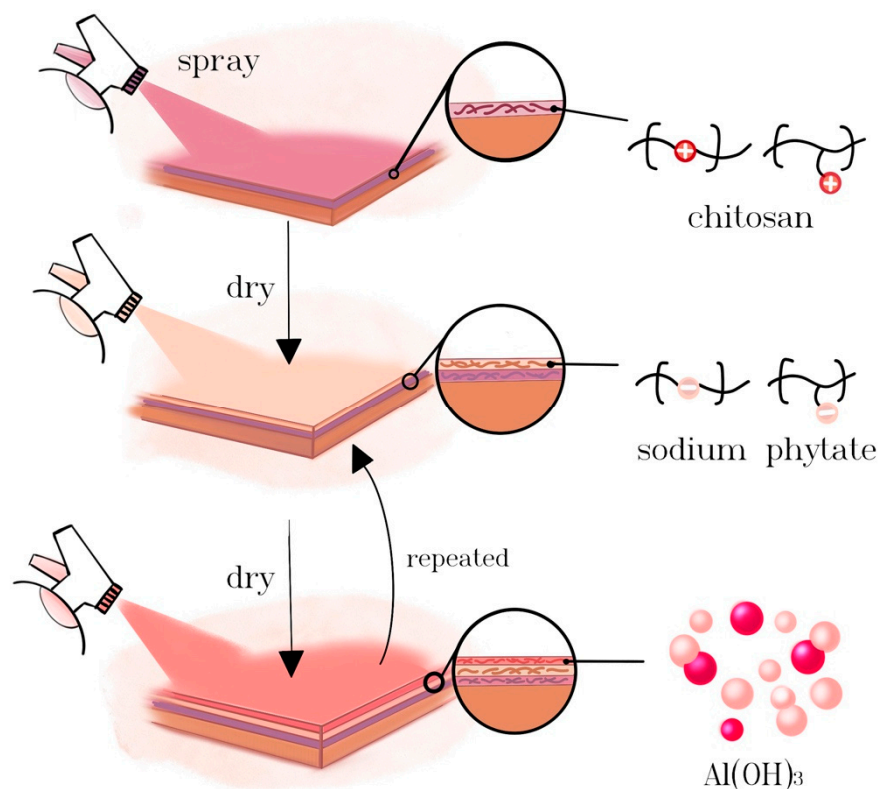


Figure 1. Scheme of fabricating chitosan/sodium phytate/Al(OH)₃ coatings on a wood surface by spray-assisted layer-by-layer self-assembly.

2.3. Characterization

2.3.1. SEM

The morphology and distribution of chitosan/sodium phytate/Al(OH)₃ loaded on the wood surface were observed by scanning electron microscopy (SEM, FEG, Quanta 400) with a scanning voltage of 20 kV under a vacuum atmosphere. The sample was cut into wood pieces at a size of 1 × 1 × 1 mm, and then an Au film of 5–10 nm thickness was coated under vacuum conditions.

2.3.2. UV Light Test

Wood samples (20 × 20 × 10 mm) were subjected to ultraviolet light-induced accelerated aging using a self-made ultraviolet lamp with a power of 48 W and a wavelength of 340 nm. The irradiation distance of the ultraviolet lamp was 10 cm with a temperature of 25 ± 1 °C. The sample had a similar surface color, and the total duration of illumination was 720 h. According to the CIE1976 color system of the International Standard Lighting

Commission, L^* (brightness), a^* (red-green index), and b^* (yellow-blue index) for each sample at certain time points before and after irradiation were measured using an HP-2136 portable colorimeter (test diameter: 8 mm) provided by Shanghai Puxi Optoelectronic Technology Co., Ltd. (Shanghai, China). Average values were calculated every five points, and the total color difference (ΔE^*) was calculated according to Equations (1)–(4) as follows:

$$\Delta L^* = L^*_s - L^*_i \quad (1)$$

$$\Delta a^* = a^*_s - a^*_i \quad (2)$$

$$\Delta b^* = b^*_s - b^*_i \quad (3)$$

$$\Delta E^* = \sqrt{\Delta L^{*2} + \Delta a^{*2} + \Delta b^{*2}} \quad (4)$$

2.3.3. Wettability Test

The water contact angle was measured using a contact angle system (CA, CAST2.0 CA analysis system (Solon Information Technology Co. Ltd., Shanghai, China) at room temperature. The volumes of the individual distilled water droplets used for the CA measurement were 5 μ L. The test solution was continuously dripped onto the wood for 1 min to analyze how the contact angle changes over time. Parameters were measured at three points on the specimen, and the average value was calculated. CA measurements were also made for the untreated wood to provide a basis for comparison.

2.3.4. Combustion Tests

Limiting oxygen index testing was conducted by an oxygen index testing apparatus (PX-01-005, Phinix, Suzhou, China) according to the standard GB2406.2-2009 with $150 \times (6.5 \pm 0.5) \times (3.0 \pm 0.5)$ mm wood samples. The apparatus was set to standard conditions, and the sample was placed vertically in the mixture of oxygen and nitrogen that had been previously adjusted to a specific value. After the airflow was stabilized, the sample was ignited. The minimum oxygen concentration required for the sample to maintain steady combustion for 3 min at 5 cm of the sample was identified as its oxygen index, which was expressed as a volume percent.

3. Results and Analysis

The structure of the original wood surface, such as vessel and pits in the vessel, appeared rough under the high-power mirror (Figure 2a). After spraying the wood with chitosan solution and the drying curing treatment, a thin film formed on the wood surface, suggesting that chitosan had been loaded on the wood surface (Figure 2b). After spraying the wood with sodium phytate solution and drying curing treatment on the exterior, the thickness of the film noticeably increased, and the structures, such as conduits on the wood surface, were further obscured, which made the wood surface smoother (Figure 2c). Finally, the $\text{Al}(\text{OH})_3$ solution was sprayed, and the wood surface was loaded with a large number of particles that were tightly arranged, which completely covered the wood surface (Figure 2d).

The accelerated ultraviolet aging test was conducted for 720 hours on the original wood and wood coated with chitosan/sodium phytate/ $\text{Al}(\text{OH})_3$. The color value before UV irradiation was used as the initial reference value to determine the color differences ΔL^* , Δa^* , and Δb^* and the total color difference ΔE^* after lighting for 2, 6, 12, 24, 36, 48, 60, 72, 96, 120, 144, 168, 192, 240, 360, 480, 600, and 720 hours. As the diagram indicates (Figure 3), the ΔL^* of the original wood was significantly reduced, and the Δa^* and Δb^* were significantly increased after 720 hours of UV exposure. The ΔL^* of CH/SP/ $\text{Al}(\text{OH})_3$ wood was opposite that of the original wood, and the Δa^* and Δb^* were the same as those of the original. Generally, the ΔL^* , Δa^* , and Δb^* of the CH/SP/ $\text{Al}(\text{OH})_3$ wood increased as the irradiation time of the ultraviolet lamp increased, but the degree of change was noticeably smaller than that of the original wood, which indicated that CH/SP/ $\text{Al}(\text{OH})_3$ coatings attached to the wood surface showed strong photostability and conferred a UV

protective effect on wood. It could be inferred that the structure of six hydroxyl groups around the Al atom enhanced the UV absorption in the specified range [34].

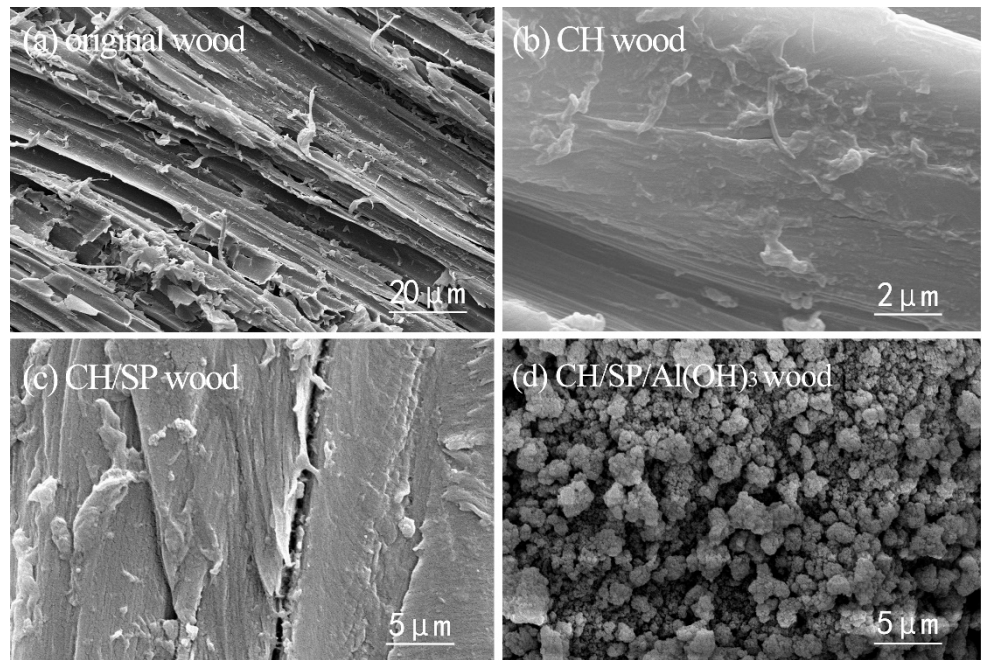


Figure 2. SEM images of (a) original wood; (b) CH wood; (c) CH/SP wood and (d) CH/SP/Al(OH)₃ wood.

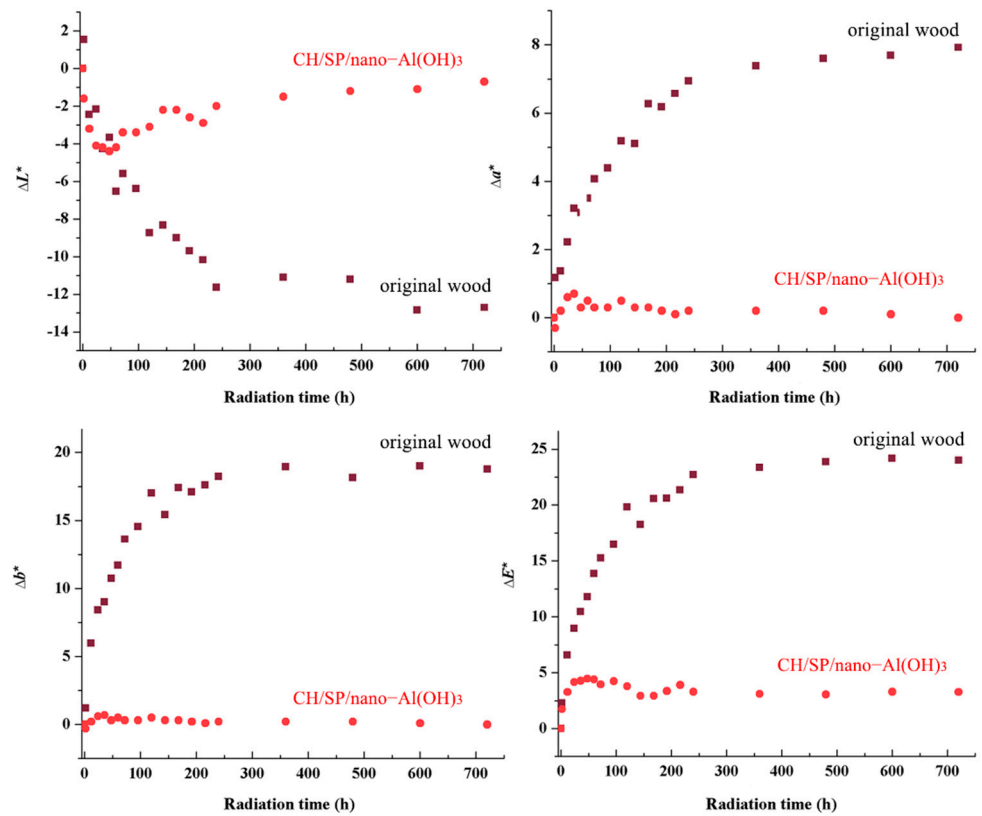


Figure 3. Changing parameters ΔL^* , Δa^* , Δb^* , and ΔE^* of the original wood and the CH/SP/Al(OH)₃ wood.

As shown in Figure 4, the initial static contact angle of the original wood was 75° , and the wood had hydrophilic characteristics. As time progressed, the water droplets gradually adsorbed into the wood interior, and the contact angle decreased to 32° after 60 s, as there were gaps on the wood surface, and tubular holes were abundant. The initial static contact angle of the CH/SP/Al(OH)₃ wood was 140° , and the wood showed high hydrophobicity. As time progressed, the contact angle decreased to 120° slowly after 60 s, and the wood still showed high hydrophobicity. These results, combined with SEM image analysis, revealed that the micro-nano structure introduced into the wood substrate induced hydrophobicity. The trapped air pressure balances the gravity of the water droplet and produces a gas layer on the wood surface, inducing the droplet to seemingly “sit” on the wood surface [35].

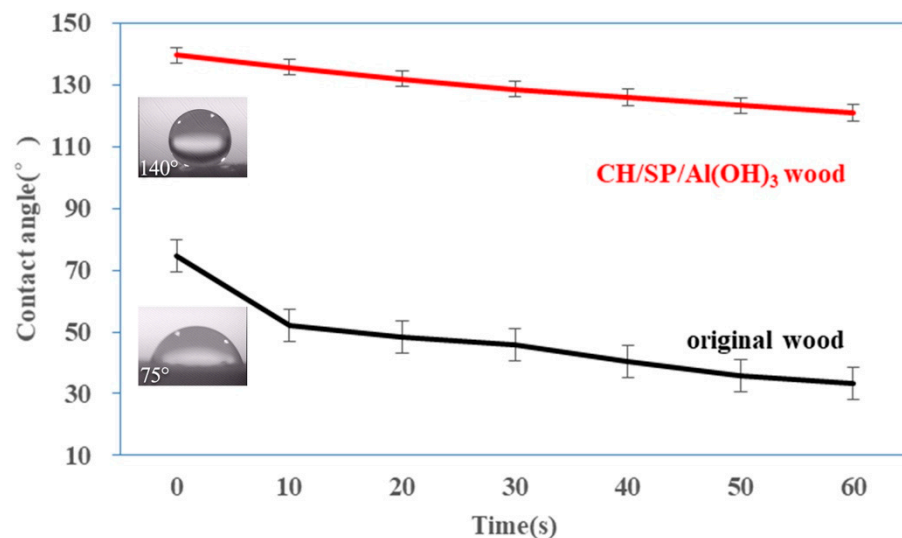


Figure 4. Water contact angles with holding time of original wood (black line) and the CH/SP/Al(OH)₃ wood (red line).

Chitosan, sodium phytate, and Al(OH)₃ were used to conduct flame-retardant finishing of the wood by electrostatic LbL self-assembly. The effect of each component on the flame-retardant properties of the wood was studied using the limiting oxygen index (LOI) for assessment (Figure 5a). The LOI value of the original wood that belonged to combustible material was 24.6. After loading chitosan on the wood surface, the LOI value increased to 26.5, and the flame retardancy was improved. This increase likely stemmed from the fact that the amine groups of chitosan became protonated under acidic conditions, resulting in high nitrogen content. Therefore, the addition of chitosan can help wood achieve better flame retardancy. After further binding of wood to sodium phytate, the LOI value noticeably increased, as the higher phosphorus content of sodium phytate can have a flame-retardant effect. After loading Al(OH)₃ on the surface of the wood, the LOI value increased to 31.2, and the wood was composed of refractory materials. This observation may stem from the release of crystalline water through the thermal decomposition of aluminum hydroxide while absorbing a large amount of heat, which can cool the combustion surface and inhibit the continuous combustion of wood. The flame retardancy of the original wood, CH wood, CH/SP wood, and CH/SP/Al(OH)₃ wood samples was assessed by direct exposure to an alcohol lamp flame to show more direct observations (Figure 5b). In this experiment, the original wood burned vigorously, and the flame spread quickly when it was ignited, finally burning to ashes. The flame spread slowly and evenly, and the surface of the specimen was gradually carbonized after the CH wood and the CH/SP wood were fired. The CH wood and the CH/SP wood automatically extinguished after tens of seconds with a slightly altered shape. CH/SP/Al(OH)₃ wood was not easy to ignite, and its flame did not easily expand; consequently, the flame automatically extinguished after 14–15 s. CH/SP/Al(OH)₃ wood showed better refractory properties, which was consistent with the

LOI measurements. Table 1 lists the description of each group and the results of statistical analysis (one-way ANOVA). It is obvious that the p -value < 0.05 , indicating that different assembly structures did have a significant impact on wood flame retardancy.

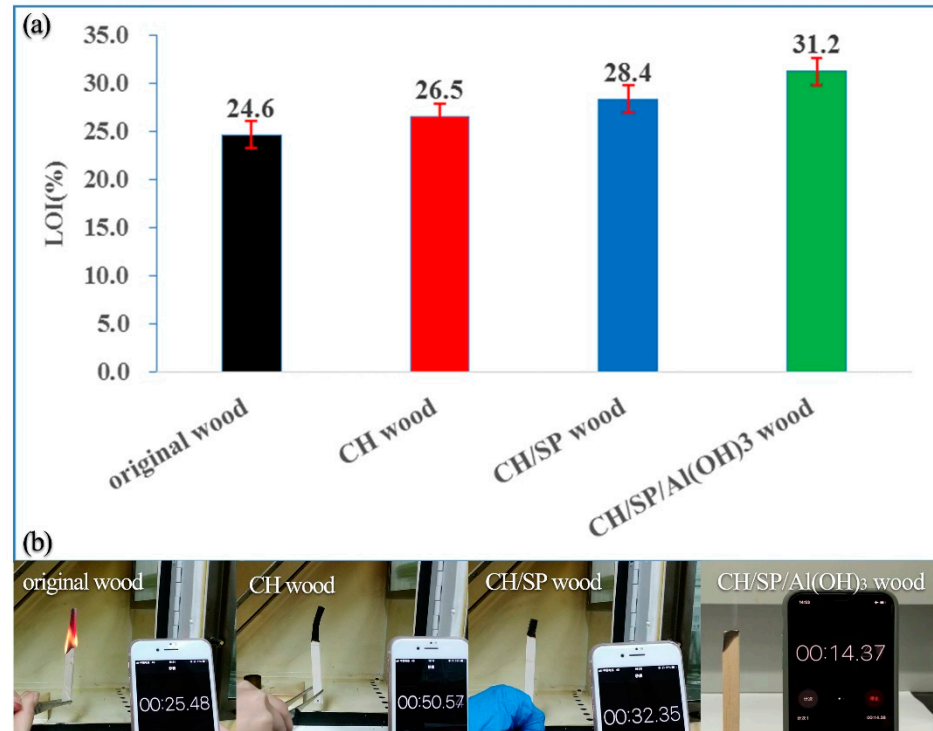


Figure 5. LOI (a) and flame burning tendency (b) of the original wood, CH wood, CH/SP wood, and CH/SP/Al(OH)₃ wood samples.

Table 1. Correlation data of self-extinguishing time and one-way ANOVA.

	Quantity	Mean	Std. Deviation	Variance		
CH	5	50.51	0.84	1.394		
CH/SP	5	31.98	1.14	2.486		
CH/SP/Al(OH) ₃	5	13.51	0.57	0.157		
ANOVA						
Sources	SS	df	MS	F	p -Value	F crit
Between groups	1368.631	2	684.3157	508.4447	0.00016	9.552094
Within groups	4.0377	3	1.3459			
Total	1372.669	5				

4. Conclusions

An efficient protective coating was obtained on the wood surface via a facile spray assisted layer-by-layer self-assembly method. Specifically, natural green chitosan and sodium phytate were used as electrolytes, aluminum hydroxide particles with positive charge were used as functional groups to achieve anti-aging, water-repellent, and flame-retardant properties. SEM images confirmed that the wood surface was completely covered by a large number of tightly arranged aluminum hydroxide particles. Moreover, the treated wood had superior UV-resistant properties compared with untreated wood. After 720 h of UV exposure, the brightness L^* , red-green index a^* , and the yellow-blue index b^* of the CH/SP/Al(OH)₃ wood increased, but the degree of change was noticeably smaller

compared with the original wood. The micro-nano structure of aluminum hydroxide created the roughness of the structure and induced hydrophobicity. The initial test static contact angle increased to 140°, and it showed high hydrophobic stability over time. LOI and air exposure combustion tests were used to verify that chitosan, sodium phytate, and aluminum hydroxide can produce significant synergistic fire resistance to modified wood. CH/SP/Al(OH)₃ wood was not easy to ignite, and its flame was resistant to expansion, which automatically extinguished after 14–15 s. Its LOI reached 31.2, and it had excellent refractory characteristics.

Author Contributions: Conceptualization, Y.W. and M.G.; methodology, Y.W. and Y.F.; software, S.H.; validation, Y.W., S.H., and M.G.; formal analysis, Y.W.; investigation, S.H.; resources, Y.W.; data curation, Y.W.; writing—original draft preparation, Y.W. and M.G.; writing—review and editing, Y.W. and Y.F.; visualization, S.H.; supervision, Y.W.; project administration, Y.W. and Y.F. All authors have read and agreed to the published version of the manuscript.

Funding: This research was funded by the General Project of Philosophy and Social Science Research in Jiangsu Universities, grant number 2019SJA0122 and the Youth Science and Technology Innovation Fund of Nanjing Forestry University, grant number CX2016016.

Institutional Review Board Statement: Not applicable.

Informed Consent Statement: Not applicable.

Data Availability Statement: Not applicable.

Acknowledgments: The authors thank Institute of Chemical Industry of Forest Products for providing invaluable technical assistance in the chemistry laboratory.

Conflicts of Interest: The authors declare no conflict of interest.

References

1. Starzak, M.; Makaruk, H.; Sadowski, J. Step Length Adjustment in the Long Jump with and without Take-off Board in non-Long Jumpers. *JKES* **2015**, *70*, 19–25.
2. Evans, P.D. Weathering of Wood and Wood Composites. In *Handbook of Wood Chemistry and Wood Composites*, 2nd ed.; Rowell, R.M., Ed.; CRC Press: Boca Raton, FL, USA, 2012; pp. 151–216.
3. Feist, W.C. Outdoor Wood Weathering and Protection. In *Archaeological Wood Properties, Chemistry, and Preservation*; Rowell, R.M., Barbour, R.J., Eds.; American Chemical Society: Washington, DC, USA, 1990; pp. 263–298.
4. Henriques, D.F.; Azevedo, A.C.B. Outdoor Wood Weathering and Protection. In *Proceeding of the 7th Rehabend Congress—Construction Pathology, Rehabilitation Technology and Heritage Management*, Caceres, Spain, 15–18 May 2018.
5. Dong, H.; Bahmani, M.; Rahimi, S.; Humar, M. Influence of Copper and Biopolymer/Saqez Resin on the Properties of Poplar Wood. *Forests* **2020**, *11*, 667. [[CrossRef](#)]
6. Chu, D.; Mu, J.; Avramidis, S.; Rahimi, S.; Liu, S.; Lai, Z. Functionalized Surface Layer on Poplar Wood Fabricated by Fire Retardant and Thermal Densification. Part 1: Compression Recovery and Flammability. *Forests* **2019**, *10*, 955. [[CrossRef](#)]
7. Rajkovic, V.J.; Bogner, A.; Radovan, D. The Efficiency of Various Treatments in Protecting Wood Surfaces against Weathering. *Surf. Coat. Int. B Coat. Trans.* **2004**, *87*, 15–19. [[CrossRef](#)]
8. Evans, P.D.; Chowdhury, M.J.; Mathews, B.; Schmalzl, K.; Syer, S.; Kiguchi, M.; Kataoka, Y. Weathering and Surface Protection of Wood. In *Handbook of Environmental Degradation of Materials*; Kutz, M., Ed.; William Andrew: New York, NY, USA, 2005; pp. 277–297.
9. Hill, C.A.S. *Wood Modification: Chemical, Thermal and Other Processes*; John Wiley & Sons Ltd.: West Sussex, UK, 2007.
10. Sandberg, D.; Kutnar, A.; Mantanis, G. Wood Modification Technologies—A Review. *IFOREST* **2017**, *10*, 895–908. [[CrossRef](#)]
11. Militz, H. Wood Modification Research in Europe. *Holzforschung* **2020**, *74*, 333. [[CrossRef](#)]
12. Schaller, C.; Rogez, D. New Approaches in Wood Coating Stabilization. *J. Coat. Technol. Res.* **2007**, *4*, 401–409. [[CrossRef](#)]
13. Windt, I.D.; Bulcke, J.V.; Wuijstens, I.; Coppens, H.; Acker, J.V. Outdoor Weathering Performance Parameters of Exterior Wood Coating Systems on Tropical Hardwood Substrates. *Eur. J. Wood Wood Prod.* **2014**, *72*, 261–272. [[CrossRef](#)]
14. Yan, X.X.; Wang, L.; Qian, X.Y. Effect of Coating Process on Performance of Reversible Thermochromic Waterborne Coatings for Chinese Fir. *Coatings* **2020**, *10*, 223. [[CrossRef](#)]
15. Ariga, K.; Hill, J.P.; Ji, Q.M. Layer-by-Layer Assembly as A Versatile Bottom-up Nanofabrication Technique for Exploratory Research and Realistic Application. *Phys. Chem. Chem. Phys.* **2007**, *9*, 2319–2340.
16. Ariga, K.; Yamauchi, Y.; Rydzek, G.; Ji, Q.M.; Yonamine, Y.; Wu, K.C.-W.; Hill, J.P. Layer-by-layer Nanoarchitectonics: Invention, Innovation, and Evolution. *Chem. Lett.* **2014**, *43*, 36–68. [[CrossRef](#)]

17. Wågberg, L.; Erlandsson, J. The Use of Layer-by-Layer Self-Assembly and Nanocellulose to Prepare Advanced Functional Materials. *Adv. Mater.* **2020**, 2001474. [[CrossRef](#)] [[PubMed](#)]
18. Agarwal, M.; Lvov, Y.; Varahramyan, K. Conductive Wood Microfibres for Smart Paper through Layer-by-layer Nanocoating. *Nanotechnology* **2006**, *17*, 5319–5325. [[CrossRef](#)]
19. Renneckar, S.; Zhou, Y. Nanoscale Coatings on Wood: Polyelectrolyte Adsorption and Layer-by-Layer Assembled Film Formation. *ACS Appl. Mater. Interfaces* **2009**, *1*, 559–566. [[CrossRef](#)] [[PubMed](#)]
20. Köklükaya, O.; Carosio, F.; Grunlan, J.C.; Wågberg, L. Flame-Retardant Paper from Wood Fibers Functionalized via Layer by-Layer Assembly. *ACS Appl. Mater. Interfaces* **2015**, *7*, 23750–23759. [[CrossRef](#)]
21. Rao, X.; Liu, Y.; Fu, Y.; Liu, Y.; Yu, H. Formation and properties of polyelectrolytes/TiO₂ composite coating on wood surfaces through layer-by-layer assembly method. *Holzforschung* **2016**, *70*, 361–367. [[CrossRef](#)]
22. Tang, T.L.; Fu, Y.C. Formation of Chitosan/Sodium Phytate/Nano-Fe₃O₄ Magnetic Coatings on Wood Surfaces via Layer-by-Layer Self-Assembly. *Coatings* **2020**, *10*, 51. [[CrossRef](#)]
23. Zhou, L.; Fu, Y.C. Flame-Retardant Wood Composites Based on Immobilizing with Chitosan/Sodium Phytate/Nano-TiO₂-ZnO Coatings via Layer-by-Layer Self-Assembly. *Coatings* **2020**, *10*, 296. [[CrossRef](#)]
24. Agriga, K.; Hill, J.P.; Lee, M.V.; Vinu, A.; Charvet, R.; Acharya, S. Challenges and Breakthroughs in Recent Research on Self-assembly. *Sci. Technol. Adv. Mater.* **2008**, *9*, 014109. [[CrossRef](#)]
25. Sekar, S.; Lemaire, V.; Hu, H.; Decher, G.; Pauly, M. Anisotropic Optical and Conductive Properties of Oriented 1D-Nanoparticle Thin Films Made by Spray-assisted Self-assembly. *Faraday Discuss.* **2016**, *191*, 373. [[CrossRef](#)]
26. Heo, J.W.; Choi, M.H.; Hong, J.K. Assisted Layer-by-Layer Self-Assembly of Graphene Oxide for Oxygen Barrier Properties. *Sci. Rep.* **2019**, *9*, 2754. [[CrossRef](#)] [[PubMed](#)]
27. Malik, N.; Dov, N.E.; Ruiter, G.d.; Lahav, M.; Boom, M.E.v.d. On-Surface Self-Assembly of Stimuli-Responsive Metallo-Organic Films: Automated Ultrasonic Spray-Coating and Electrochromic Devices. *ACS Appl. Mater. Interfaces* **2019**, *11*, 22858–22868. [[CrossRef](#)] [[PubMed](#)]
28. Schlenoff, J.B.; Dubas, S.T.; Farhat, T. Sprayed Polyelectrolyte Multilayers. *Langmuir* **2000**, *16*, 9968–9969. [[CrossRef](#)]
29. Shi, H.; Xue, L.; Gao, A.; Fu, Y.; Zhou, Q.; Zhu, L. Fouling-resistant and adhesion-resistant surface modification of dual layer PVDF hollow fiber membrane by dopamine and quaternary polyethyleneimine. *J. Membr. Sci.* **2016**, *498*, 39–47. [[CrossRef](#)]
30. Kai, C.; Catchmark, J.M. Improved eco-friendly barrier materials based on crystalline nanocellulose/chitosan/carboxymethyl cellulose polyelectrolyte complexes. *Food Hydrocoll.* **2018**, *80*, 195–205.
31. Nikolaeva, M.; Käerki, T. Influence of mineral fillers on the fire retardant properties of wood-polypropylene composites. *Fire Mater.* **2013**, *37*, 612–620. [[CrossRef](#)]
32. Yan, W.; Wang, K.; Huang, W.; Wang, M.; Tian, Q. Synergistic effects of phenethyl-bridged doped derivative with Al(OH)₃ on flame retardancy for epoxy resins. *Polym-Plast. Technol. Mat.* **2019**, *59*, 1–12. [[CrossRef](#)]
33. Guo, F.X.; Lei, L.I.; Zhou, Z.H.; Wang, Q.W.; Yi-Meng, H.U. Hydrophobic Modification of PP Membrane Coated by Al(OH)₃ Colloids. In Proceedings of the 3rd International Conference on Material Engineering and Application (ICMEA 2016), Shanghai, China, 12–13 November 2016; pp. 205–209.
34. Wang, N.N.; Fu, Y.C.; Liu, Y.Z.; Yu, H.P. Synthesis of aluminum hydroxide thin coating and its influence on the thermomechanical and fire-resistant properties of wood. *Holzforschung* **2014**, *68*, 781–789. [[CrossRef](#)]
35. Fu, Y.C.; Yu, H.P.; Sun, Q.F.; Li, G.; Liu, Y.X. Testing of the superhydrophobicity of a zinc oxide nanorod array coating on wood surface prepared by hydrothermal treatment. *Holzforschung* **2012**, *66*, 739–744. [[CrossRef](#)]